Developing hyperpolarized metabolic contrast agents at high field dDNP for large animal research

Christensen, Ditte B.; Skre, Ingeborg S.; Ardenkjær-Larsen, Jan Henrik; Karlsson, Magnus; Lerche, Mathilde H.

Published in:
Journal of Magnetic Resonance Open

Link to article, DOI:
10.1016/j.jmro.2024.100184

Publication date:
2025

Document Version
Publisher's PDF, also known as Version of record

Citation (APA):
Christensen, D. B., Skre, I. S., Ardenkjær-Larsen, J. H., Karlsson, M., & Lerche, M. H. (2025). Developing hyperpolarized metabolic contrast agents at high field dDNP for large animal research. *Journal of Magnetic Resonance Open*, *22*, Article 100184. https://doi.org/10.1016/j.jmro.2024.100184

Journal of Magnetic Resonance Open 22 (2025) 100184

Contents lists available at ScienceDirect

Journal of Magnetic Resonance Open

journal homepage: www.sciencedirect.com/journal/journal-of-magnetic-resonance-open

Developing hyperpolarized metabolic contrast agents at high field dDNP for large animal research

Ditte B. Christensen [1], Ingeborg S. Skre [1], Jan Henrik Ardenkjær-Larsen, Magnus Karlsson, Mathilde H. Lerche *

Center for Hyperpolarization in Magnetic Resonance, Department of Health Technology, Technical University of Denmark, Kgs. Lyngby, Denmark

ARTICLE INFO

Keywords:
13C-Hyperpolarization
MRS, Large animal research
2-keto-isocaproate
Fumarate

ABSTRACT

Dissolution Dynamic Nuclear Polarization (dDNP) polarizers have achieved high field strengths and large sample volumes. These advancements necessitate new formulations of hyperpolarized metabolic contrast agents (HMCAs) to enable large animal studies. While several metabolic substrates have been investigated at lower field dDNP and tested as HMCAs in rodents, ^{13}C-labeled pyruvate remains the most studied HMCA and is currently the only one actively used in clinical trials due to its favorable biological and physical properties. Effective human and large animal dDNP formulations require high molar substrate concentrations, low DNP sample viscosity for efficient dissolution, and adequate dilution of the DNP sample to minimize signal decay and maximize HMCA concentration.

We present substrate formulations optimized for high-field polarization and large-volume dissolution. Specifically, we validate the upscaling of [1–^{13}C]pyruvate under high-field conditions and demonstrate that [1–^{13}C] 2-keto-isocaproate and [1,4–^{13}C$_2$]fumarate, which have been proven successful in rodent studies, can be formulated to yield high polarization at suitable concentrations and volumes for large animal metabolic MR imaging.

Introduction

With the advent of ^{13}C hyperpolarization, dynamic metabolic magnetic resonance imaging (MRI) has evolved into a powerful modality for non-invasive detection and analysis of both normal and abnormal cellular metabolism [1]. The ability to dynamically track metabolic changes allows insights into various physiological and pathological states, offering value for diagnosing diseases [2], monitoring treatment efficacy [3] and conducting mechanistic metabolic research [4].

The strengths of ^{13}C-hyperpolarized metabolic MRI lie in its use of endogenous compounds with well-documented biochemistry, toxicology, and pharmacokinetics, ensuring safety and reliability in clinical applications. Additionally, the technique excels in differentiating enzymatically generated metabolic products spatially and temporally from their substrates. This capability allows for precise mapping of metabolic processes and real-time tracking of biochemical transformations within the body.

Comprehensive studies have optimized DNP sample formulations for a broad selection of hyperpolarized metabolic contrast agents (HMCAs) for polarization at 3.35 T [5]. While several HMCAs have proven effective in rodent models [6], only hyperpolarized ^{13}C-pyruvate (PYR) has been studied in pig models [7,8] and is currently the only HMCA actively used in human clinical research [9].

Meeting the demands for viable HMCAs for large animal and human use involves ensuring fast and effective MR imaging of metabolite signals well separated in chemical shift from the signals of their HMCA origin. To allow sufficient HMCA signal following dilution in circulation, 10–50 mL highly polarized HMCAs in 80–250 mM concentrations with suitable pH, temperature and tonicity are needed. Therefore, high molar concentrations in vitrifying solutions are necessary to produce sufficiently concentrated liquid-state DNP samples for injection. A notable advantage of pyruvate as an HMCA for large animal and human clinical research is that its acid form, pyruvic acid, is a highly concentrated liquid at room temperature (14M), and an excellent vitrifying liquid that allows for the preparation of PYR for hyperpolarization without additional solvents.

* Corresponding author.
E-mail address: mhauler@dtu.dk (M.H. Lerche).

[1] Equal contribution.

https://doi.org/10.1016/j.jmro.2024.100184

Available online 27 December 2024

Due to the many physical and biological demands, only few HMCAs are likely candidates for translation into large animal and human clinical research. Notable HMCAs such as [1–^{13}C]2-ketoisocaproate (KIC) and [1,4–$^{13}C_2$]fumarate (FUM), previously studied pre-clinically in rodents [10,11,12], are promising candidates for large animal and human research owing to their critical involvement in central metabolic pathways. For instance, KIC plays a pivotal role as an intermediate in branched-chain amino acid metabolism, linking energy production with protein turnover, while fumarate is a key component of the tricarboxylic acid (TCA) cycle, which is essential for cellular energy production and metabolic homeostasis. These intrinsic biological functions, combined with their fast metabolic kinetics, make KIC and FUM particularly attractive for clinical translation.

To hyperpolarize the DNP sample and produce an injectable hyperpolarized liquid - the HMCA, a dissolution Dynamic Nuclear Polarization (dDNP) polarizer is required. Direct ^{13}C hyperpolarization is achieved by microwave-mediated transfer of polarization from stable radicals mixed with ^{13}C labeled compounds at high field (typically 3–7 T) and low temperature (typically below 1.5 K) conditions. This process, though slow with tens of minutes-long polarization build-up time, typically yields more than 10 % ^{13}C polarization. The polarization build-up time (T_p) depends on DNP sample composition, particularly the concentration of radicals and the concentration of ^{13}C spins [5].

Commercially available clinical and pre-clinical dDNP polarizers are cryogen-free and operate at increased field strengths (5–7T) and/or lowered temperatures (0.8–1.3K) [13,14]. This facilitates higher ^{13}C polarization than the original prototype polarizers, achieved mainly due to a field strength dependent decrease in the T_1 of the unpaired electron of the stable radicals that are used as electron polarizing agent (EPAs) [15]. Optimizing DNP sample compositions to achieve fast and high polarization is an experimental task.

A limiting condition for dDNP polarizers is the available sample space, which, dependent on the specific design, allows for polarizing up to 2 ml DNP sample [16,17,14,18]. Dissolution of the frozen DNP sample with a heated dissolution medium is needed to produce the HMCA. Producing an injectable solution by reproducibly bringing a large DNP sample volume from approximately 1.3K to 310 K requires a suitable volume of dissolution medium. Optimizing sample dissolution conditions to yield full sample recovery, retaining polarization, and minimizing unfavorable relaxation effects is an experimental task. Given the technical challenges of achieving both high polarization levels and short polarization build-up times for large-volume, high-concentration samples suitable for large-animal and human studies, this work focuses on optimizing Tritryl radical concentration as a practical and scalable solution.

In this work, we demonstrate how KIC and FUM can be hyperpolarized at 6.7T to levels comparable to PYR and formulated in concentrations and volumes suitable for large animal studies.

We investigate the benefits of hyperpolarizing PYR using direct ^{13}C polarization at 6.7T compared to lower field, and we study the dependence of polarization level on EPA concentration and on ^{13}C spin concentration. We use these insights to optimize polarization at 6.7T for KIC and FUM and to scale up the sample sizes for these HMCAs to target large animal studies. Lastly, we test the formulation of KIC by using it as an HMCA injected intravenously in a pig and measuring ^{13}C dynamic spectra over the pigś head.

Results and discussion

Fast High-Field Polarization of [1–^{13}C]PYR

Direct carbon polarization with dDNP hyperpolarized [1–^{13}C]PYR was initially developed at 3.35T and approximately 1.3K, achieving about 20 % polarization at an optimized EPA concentration [19]. Using an EPA enhancer, typically a paramagnetic compound containing Gd, reduces the electron T_1 (T_1e) of the EPA [20] enabling a polarization of 35±5 % for [1–^{13}C]pyruvic acid at 3.35T and approximately 1.3K [5]. Increasing the magnetic field strength also reduces the T_1e, allowing for even higher polarization levels (60.4±4.7 % at 7 T and 1 K), but at the cost of a higher build up constant (T_p). While T_p can be reduced by increasing the EPA concentration, at 7T, adding EPA enhancer does not significantly affect the polarization of [1–^{13}C]PYR [21].

We have compared polarization obtained for [1–^{13}C]PYR as a function of trityl EPA concentration at 3.35 T and 6.7 T and approximately 1.3 K, Fig. 1. The given polarization measurements are liquid state polarization measured 10s after dissolution.

At both field strengths the time it takes to build up polarization is inversely and strongly dependent on the EPA concentration. At 6.7T the polarization optimum is flat over a 20 mM EPA concentration interval. In this interval the corresponding T_p decreases from approximately 60 to 20 minutes. Although our commonly used EPA concentration at high field is 30 mM, we also investigated very high EPA concentrations (58 mM) where 35 % polarization could be obtained in 25 min (T_p of 9±2 min). Increasing the EPA concentration is clearly a good strategy to reduce polarization time at 6.7T, if the EPA concentration after dissolution does not affect the liquid state T_1. With a dilution factor of 180, no effect was measured on a 80 mM [1–^{13}C]PYR T_1 (60±3s at 9.4T, 38±2 C) in DNP samples with solid state trityl EPA concentrations in the interval 20–60 mM.

The effect of adding an EPA enhancer in the form of the clinically used Gd contrast agent Prohance was highly significant (35±3 % versus 20±2 %) at 3.35 T with 15 mM EPA, whereas no effect was observed on the polarization at 6.7T with 30 mM EPA (47±4 % versus 48±2 %).

At 6.7T, lowering the percentage of ^{13}C isotopic enrichment prolonged T_p and resulted in lower end-polarization. However, this could be compensated for with higher EPA concentrations, Fig. 2.

A mixture of 10 % isotope labeled [1–^{13}C]PYR in non-isotope labeled PYR with 58 mM EPA could be polarized to 37 % in one hour. This is similar to the end-polarization for a 99 % isotope-labeled DNP sample, though with a doubled T_p. Adding EPA enhancer increased the polarization of this sample with a factor of 1.2, though at the expense of a longer T_p. Non-isotope enriched [1–^{13}C]PYR was highly polarized at this EPA concentration (32 % after 1.5 hours), approximately a factor of 0.85

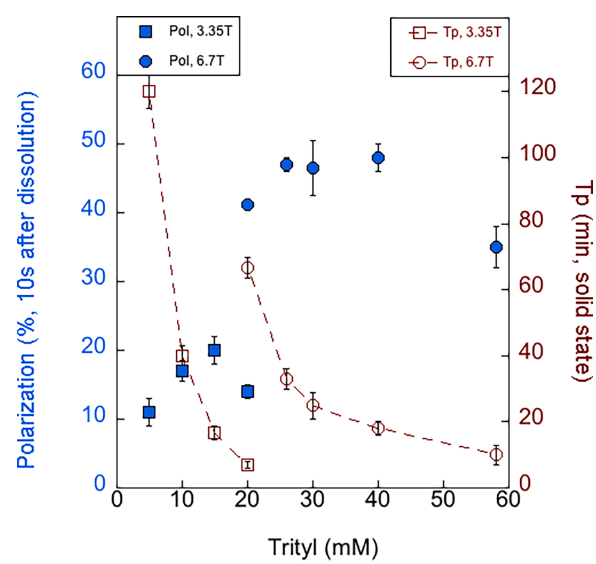

Fig 1. Hyperpolarization of [1–^{13}C]PYR. Polarization (Y1 axis, blue) was measured in liquid state (9.4T, 37C) 10s after dissolution. Solid squares represent polarization measurements at 3.35T and 1.3K. Solid circles represent measurements at 6.7T and 1.3 K. The time it takes to build the hyperpolarization in the solid state is given by the polarization time constant (T_p, Y2 axis, red), at 3.35T (open squares) and at 6.7T (open circles). The DNP samples have been polarized for three time-constants to achieve 95 % of the available polarization (3x T_p). Dashed lines are included to enhance visibility.

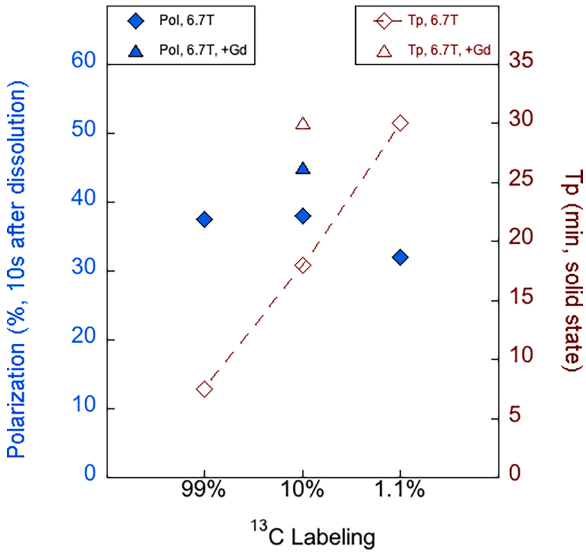

Fig 2. Hyperpolarization of [1–^{13}C]PYR at different degrees of ^{13}C labeling. Polarization (Y1 axis, blue) was measured in liquid state (9.4T, 37C) 10s after dissolution. Solid diamonds represent polarization measurements at 6.7T and 1.3 K of [1–^{13}C]PYR prepared with 58 mM EPA. The time it takes to build the hyperpolarization in the solid state is given by the polarization time constant (T_p, Y2 axis, red) at 6.7T (open diamonds). Effect of EPA enhancer for a [1–^{13}C] PYR sample with 10 % isotope labeling is shown as a solid triangle (polarization) and as an open triangle (T_p). 95 % of the available polarization is reached within 3x T_p. The dashed line is included to enhance visibility.

compared to the 99 % isotope enriched [1–^{13}C]PYR but with a 4 times longer T_p.

Overall, it is favorable to polarize pyruvic acid at high field (6.7T) and at higher EPA concentration where about 40 % polarization can be reached in approximately 25 min. Under these conditions, the high concentration (14M) allows for efficient polarization of non-isotope-enriched pyruvic acid.

High-Field Polarization of [1–^{13}C]KIC and [1,4–$^{13}C_2$]FUM

Polarization of [1–^{13}C]KIC and [1,4–$^{13}C_2$]FUM, like [1–^{13}C]PYR, was initially developed at 3.35T and approximately 1.3K [5]. KIC is a liquid at room temperature with a concentration of 8M. Conversely, FUM is a solid compound with low solubility in most solvents, but can dissolve to 3.5 M in DMSO when mixed in a 2:1 ratio. Both compounds can form a stable glass and can be highly polarized at 3.35T [5]. Polarization levels using EPA enhancers were notable reaching 32±3 % polarization for [1–^{13}C]KIC with 11 mM EPA, [10] and 31±5 % for [1,4–$^{13}C_2$]FUM with 13 mM EPA, [12].

We have compared the hyperpolarization obtained for [1–^{13}C]KIC and [1,4–$^{13}C_2$]FUM as a function of EPA concentration at 3.35T and 6.7T and approximately 1.3 K, as shown in Figs. 3A and 3B.

At 6.7T and 1.3K, [1–^{13}C]KIC achieved an optimum polarization of 52±2 % at an EPA concentration of 25 mM, without the use of EPA enhancers. High polarization 40±2 % could be achieved faster within 25 minutes, at an EPA concentration of 40 mM. The addition of an EPA enhancer further improved the polarization; at 40 mM EPA, the polarization increased to 50 %±4, although T_p was extended from 8±2 minutes to 19±3 minutes. With a dilution factor of 100, no effect was measured on the liquid state T_1 (56±1s at 9.4T, 38±2 C) for [1–^{13}C]KIC (80 mM) in samples with solid state trityl EPA concentrations ranging from 20–40 mM.

In contrast, hyperpolarization of [1,4–$^{13}C_2$]FUM showed no optimum with EPA concentration, unlike [1–^{13}C]KIC and [1–^{13}C]PYR. The polarization performance of [1,4–$^{13}C_2$]FUM was generally more sensitive to EPA concentration. Increasing the EPA concentration beyond 35 mM significantly reduced polarization, while reducing the EPA concentration resulted in a linear increase in maximum polarization. For example, at 25 mM EPA, the polarization reached 39±2 %, but the T_p was significantly prolonged to 50±2 minutes. The addition of an EPA enhancer further improved the polarization; at 30 mM EPA, the polarization increased from 33±3 % to 43±3 %, although T_p was extended from 17±2 minutes to 45±5 minutes. These findings suggest that optimizing EPA concentration for [1,4–$^{13}C_2$]FUM is more challenging than for [1–^{13}C]KIC, and its performance may vary based on experimental requirements.

Large Volume, High Concentration HMCA

The available signal in a metabolic MR exam is a composite of the amount (concentration and volume) of metabolic substrate and polarization. High polarization achieved within a practical time frame is thus only one of two requirements when producing HMCAs for large animal and human metabolic studies. For the substrate amount, highly concentrated liquids are ideal, because the sample space in a polarizer is

3A 3B

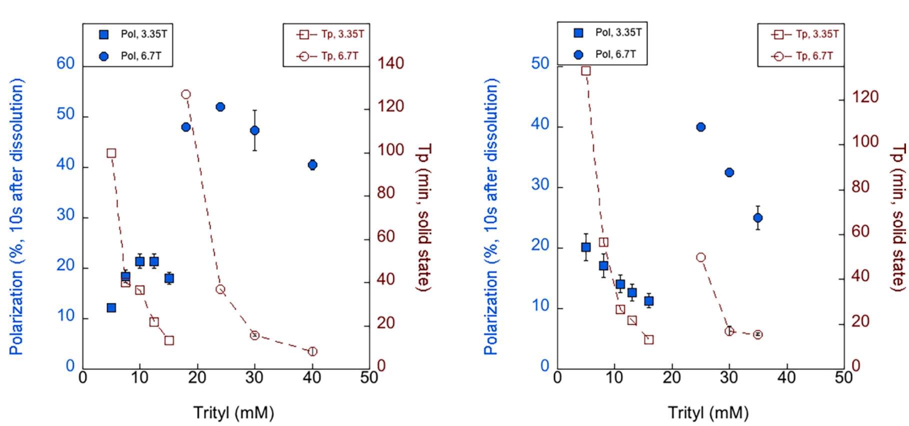

Fig 3. Hyperpolarization of [1–^{13}C]KIC (A) and [1,4–$^{13}C_2$]FUM (B). Polarization (Y1 axis, blue) was measured in liquid state (9.4T, 37C) 10s after dissolution. Solid squares represent measurements at 3.35T and 1.3K. Solid circles represent measurements at 6.7T and 1.3 K. The time to build the hyperpolarization in the solid state is given by the polarization time constant (T_p, Y2 axis, red), at 3.35T (open squares) and at 6.7T (open circles). The DNP samples have been polarized for three time-constants to achieve 95 % of the available polarization (3x T_p). Dashed lines are included to enhance visibility.

limited. All documented dDNP polarizers use the same dissolution mechanic: sample dilution with hot solvent [22]. A large dilution of the sample is beneficial to maximize the available liquid state signal by reducing the EPA concentration and minimizing its paramagnetic relaxation effect as well as to control sample temperature, pH and tonicity.

To study DNP sample amounts of [1–^{13}C]KIC and [1,4–$^{13}C_2$]FUM relevant for large animal studies in an affordable setup, we investigated the use of 10 % isotope labeled compound mixtures. As seen for [1–^{13}C]PYR, in Fig. 2, the achieved end-polarization in DNP samples with 10 % isotope labeling was identical to samples with 99 % isotope-labeled compounds, though with a longer T_p, Table 1.

The maximum volume available in our polarizer sample space was 800 μL. This allowed a maximum [1,4–$^{13}C_2$]FUM preparation of 960 mg (corresponding to 5.5 mmol ^{13}C) and 800 mg preparation of [1–^{13}C]KIC (corresponding to 6.2 mmol ^{13}C). A target volume of 30 ml was chosen to allow sufficient volume and concentration to be injected into a large animal and to dilute the DNP samples sufficiently for minimal EPA relaxation effects, good control of sample temperature and pH as well as a well-matched tonicity in the injected sample. The dissolution was performed in two steps. In the first step, the sample was dissolved in approximately 10 ml, and in the second step, the dissolved substrate was mixed with an additional 20 ml solvent to produce the final HMCA. The total dilution factors along with accounts of achieved polarizations and T_1 can be seen in Table 2.

All DNP samples were fully dissolved with 10 ml solvent. Using 30 mM EPA, it was needed to further dilute the large [1–^{13}C]KIC to avoid reduction of T_1 due to the high concentration of EPA. The T_1 of [1–^{13}C]KIC dissolved in 10 ml containing approximately 2.3mM radical was 27s, by removing EPA from the sample, the T_1 was prolonged to 36s. By diluting the KIC-concentration to 175mM, the T_1 was further prolonged to 41s.

At high field the T_1 of [1–^{13}C]KIC and [1,4–$^{13}C_2$]FUM was strongly dependent on concentration with a T_1 reduction for [1–^{13}C]KIC from 56 ±1s at about 80 mM to 45±2s at about 150 mM and for [1,4–$^{13}C_2$]FUM from 44±2s at about 40 mM to 32±2s at about 90 mM. This substrate concentration dependent T_1 likely contributes to the significantly lower liquid-state polarization in the larger concentration samples: [1–^{13}C]KIC larger DNP sample (33±2 %) compared to the smaller DNP samples (47 ±3 %), [1,4–$^{13}C_2$]FUM larger DNP sample (25±2 %) compared to the smaller DNP samples (32±3 %). It may be preferable to dissolve the samples directly in 30 ml to increase dissolution temperature and avoid sample transitions with shorter T_1.

Flux of Hyperpolarized KIC through BCAT Catalyzed Reaction in the Pig Head

The feasibility of using [1–^{13}C]KIC as an HMCA for large-animal spectroscopic imaging was demonstrated, achieving sufficient polarization level, T_1 and dose to enable dynamic in vivo spectroscopy in pigs. Hyperpolarized [1–^{13}C]KIC is metabolized to [1–^{13}C]leucine by the branched-chain amino acid aminotransferase (BCAT). This reaction was dynamically monitored in the head of a pig after intravenous administration of 30 mL hyperpolarized 140 mM [1–^{13}C]KIC (P=31 %, T_1=67s at 1.4T), pH 8 with a calculated tonicity of 480 mOsm, Figs. 4A and 4B. The signal amounts were comparable to those obtained for [1–^{13}C]PYR in the same animal, (supporting materials, Figure S1). In a summed spectrum (sum of 15 spectra over 30s), Fig. 4C, it can be seen that the signal separation at 3T between [1–^{13}C]leucine and [1–^{13}C]KIC is sufficient for a future development of fast imaging sequences for this metabolic reaction [23]. The dynamics show the build-up of [1–^{13}C]leucine, with a time-to-peak of 20s after the beginning of the injection (Supporting materials, Figure S2).

BCAT reversibly catalyzes a transfer of the branched-chain amino acid amino group to 2-ketoglutarate, forming glutamate and the respective branched-chain 2-keto acid. Specifically in the brain, KIC metabolism supports brain nitrogen homeostasis [24]. KIC has previously shown potential as an HMCA in rodent studies for cancer applications [10] and for probing neuro metabolism [11]. While [1–^{13}C]KIC is effectively metabolized in the anesthetized rodent brain, the amount of KIC metabolism across the blood-brain barrier in the propofol-anesthetized pig was limited. The detected [1–^{13}C]leucine signal was seen with MRSI to originate from the big cheek muscle in the pigś head (data not shown). A second injection with [1–^{13}C]PYR showed similarly limited uptake of this HMCA in the anesthetized pig brain.

Time domain fitted metabolite amplitude signals from the FIDs showed comparable in vivo signal amounts and an apparent in vivo T_1 of approximately 10s and 15s for [1–^{13}C]KIC and [1–^{13}C]PYR, respectively (supporting material, Figure S3). A lower injected concentration (about 100 mM) of both [1–^{13}C]KIC and [1–^{13}C]PYR was also tested in the same pig, resulting in similar substrate signal amounts and dynamics (Supporting material, Figure S4). Based on these findings it could be important to include a dose-response study in pigs in future large animal studies with [1–^{13}C]KIC.

Table 1
Effect of Decreased Isotope Labeling in Samples Prepared with 30 mM EPA. P (%): Polarization 10s after dissolution; T_p (min): Polarization build-up constant; Measurements at 6.7T and 1.3±0.05K.

MCA	100 % labeled, small sample size		10 % labeled, small sample size	
	P (%)	T_p (min)	P (%)	T_p (min)
[1–^{13}C]PYR	46±4	25±4	47±2	57 ±2
[1–^{13}C]KIC	47±3	16±1	46±4	77±4
[1,4–$^{13}C_2$]FUM	32±3	17±2	25±1	85±4

Table 2
Large Samples Prepared with 30 mM EPA. P (%): Polarization 12s after dissolution; T_1 (s): at 9.4T and approximately 38±2 C; Substrate Conc.(mM): MCA concentration in 30 ml; pH: at 37 C; mOsm: calculated tonicity; DF=sample dilution factor. Polarization at 6.7 T and 1.3±0.05K.*99 % isotope labeled compounds. **10 % isotope labeled compound.

MCA	P (%)	T_1 (s)	Conc. (mM)	pH	mOsm	DF
[1–^{13}C]PYR*	46±2	60±1	144±6	8.2±0.3	500	100
[1–^{13}C]KIC**	33±2	45±2	145±5	8.3±0.2	500	40
[1,4–^{13}C]FUM**	25±2	32±2	88±4	8.4±0.4	560	40

Conclusion

This work present recipes for highly polarized formulations of [1–^{13}C]2-ketoisocaproate and [1,4–$^{13}C_2$]fumarate that can be useful for large animal experiments. Both HMCAs were hyperpolarized in less than 1 hour to more than 25 % polarization in large volume (30 ml) and concentration (90 mM [1,4–$^{13}C_2$]FUM and 150 mM [1–^{13}C]KIC).

For [1–^{13}C]KIC, the dissolution process requires a dilution of the DNP sample of more than 35 times. This dilution is necessary to prevent negative impact on the liquid state T_1 due to high EPA concentration, high metabolic substrate concentration and low sample temperature. This formulation could also be suitable for clinical research, where it would be beneficial and straightforward to remove the EPA during the dissolution process. Due to the very low solubility of fumaric acid in water, removing EPA remains a research challenge before the [1,4–$^{13}C_2$]FUM formulation can be applied in clinical settings.

Optimization of hyperpolarization at 6.7T was found to be dependent on the formulation of the DNP sample. For [1,4–$^{13}C_2$]FUM, hyperpolarization is almost linearly dependent on EPA concentration. In contrast [1–^{13}C]KIC and [1–^{13}C]PYR exhibit a DNP optimum: for [1–^{13}C]KIC, this optimum is stable over a range of about 20 mM, while for [1–^{13}C]PYR, it is stable over about 40 mM. The broad DNP optimum for [1–^{13}C]KIC and [1–^{13}C]PYR makes it preferable to hyperpolarize

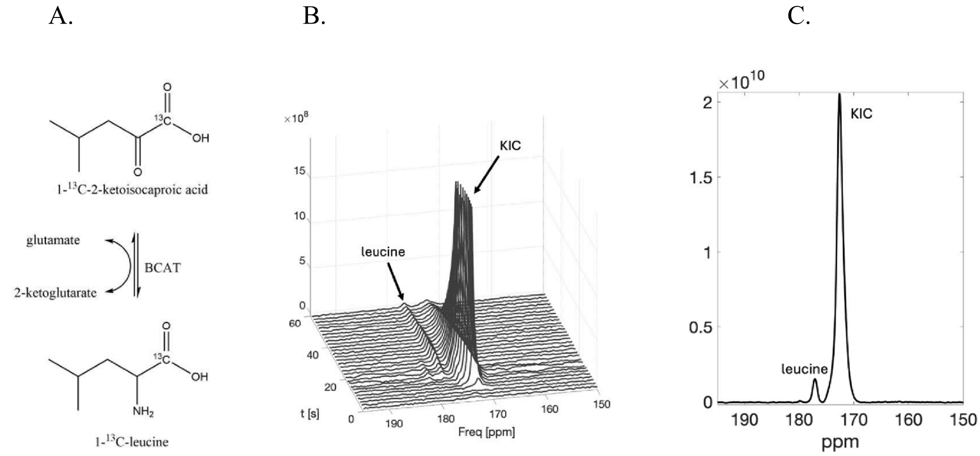

Fig 4. Flux of Hyperpolarized [1–^{13}C]KIC through the BCAT Catalyzed Reaction to [1–^{13}C]Leucine in vivo in the Pig Head. Reaction scheme for the metabolic production of [1–^{13}C]Leucine from [1–^{13}C]KIC (A) Time course of [1–^{13}C]KIC metabolic MRS in the head of a pig (B) Sum of spectra over 30s (C). MR spectra were recorded over the entire pig head every 2s with a 10 degree flip angle.

these compounds at higher EPA concentrations where polarization times are shorter.

Materials and methods

Pyruvic acid (1–^{13}C, 99 %), fumaric acid (1,4–^{13}C, 99 %) and DMSO (99 %) was purchased from Sigma-Aldrich. Trityl EPA AH111501 were obtained from GE Healthcare and Gadoteridol Gd chelate was obtained from Bracco Imaging.

[1–^{13}C]2-Ketoisocaproate, sodium salt (1–^{13}C, 99 %) was purchased from Cambridge Isotope Laboratories.

DNP sample (DS) formulations:

Definitions

DS1 (99 % isotope labeled, small sample at 3.35T or at 6.7T), DS2 (10 % isotope labeled, small sample at 6.7T), DS3 (10 % isotope labeled, large sample at 6.7T), DS4 (99 % isotope labeled, large sample at 6.7T)

EPA, AH111501: Tris(8-carboxy-2,2,6,6-(tetra(methoxyethyl)benzo-[1,2–4,5']bis-(1,3)dithiole-4-yl)methyl sodium salt, molecular weight: 1529.1 g/mol

EPA enhancer, Gadoteridol. Where applied the EPA enhancer was added to a concentration of 1.5 mM from diluted solutions of Gadoteridol in water or in DMSO.

[1–^{13}C] pyruvic acid

An example preparation of pyruvic acid with 30 mM EPA

To [1–^{13}C]PYR, 89 g/mol (100 µL, 128 mg) was added EPA (4.6 mg, 3.0 µmol AH111501). Resulting in an EPA concentration of 30 mM.

Amount for small DNP sample: approximately 18 µL, 23 mg

Amount for large DNP sample: approximately 300 µL, 384 mg

100 % isotope labeled small DNP sample for 3.35T

To [1–^{13}C]PYR (100 µL, 128 mg) was added EPA to a final concentration of either 5 mM, 10 mM, 15 mM or 20 mM. Sample amounts corresponding to small DNP samples were transferred to sample cup and inserted into the polarizer.

100 % isotope labeled small DNP sample for 6.7T

To [1–^{13}C]PYR (100 µL, 128 mg) was added EPA to a final concentration of either 20 mM, 26 mM, 30 mM, 40 mM or 58 mM. Sample amounts corresponding to small DNP samples were transferred to sample cup and inserted into the polarizer.

10 % isotope labeled small DNP sample for 6.7T

[1–^{13}C]PYR (10 µl, 12.8 mg) was mixed with PYR (90 µl, 114.3 mg). To this mixture was added EPA (4.8 mg, 3.0 µmol)resulting in an EPA concentration of 30 mM) or EPA (9.25 mg, 5.8 µmol) resulting in an EPA concentration of 58 mM. Sample amounts corresponding to small DNP samples were transferred to sample cup and inserted into the polarizer.

Non-isotope labeled small DNP sample for 6.7T

To PYR (18.5 µL, 23.7 mg) was added EPA (1.7 mg, 1.06 µmol). Resulting in an EPA concentration of 58 mM.

10 % isotope labeled large DNP sample for 6.7T

[1–^{13}C]PYR (30 µL, 38.4 mg) was mixed with PYR (270 µL, 343 mg). To this mixture was added EPA (14.4 mg, 9.0 µmol) resulting in an EPA concentration of 30 mM.

100 % isotope labeled large DNP sample for 6.7T

To [1–^{13}C]PYR(300 µL, 384 mg) was added EPA (14.4 mg, 9.0 µmol AH111501)resulting in an EPA concentration of 30 mM.

[1–^{13}C] 2-keto isocaproic acid:

[1–^{13}C]KIC is not readily commercially available in its carboxylic acid form but is sold as its sodium salt. This salt is not suitable for making dDNP sample preparations. We converted the sodium salt form to the carboxylic acid form by a simple extraction from an acidified aqueous solution of the salt. In this procedure, it is inevitable that some water will be extracted together with the KIC, in part due to the formation of the hydrate form of KIC in low pH aqueous solutions. For use in preparations for dDNP this residual water is not a problem *per se*, and it can be easily quantified by simple ^{1}H NMR spectroscopy. We commonly reach approximately 1 molecules of water per molecule KIC. The residual water has no effect on the dDNP sample properties.

Procedure

Sodium [1–^{13}C]KIC (500 mg, 3.26 mmol) was dissolved in diluted hydrochloric acid (10 ml, 2M). The solution was extracted with diethyl ether (25 ml) four times. The combined ether phases were dried over anhydrous sodium sulfate. After decanting from the solids, the solvent was evaporated on a rotavapor at 11 mbar. The recovered yield of [1–^{13}C]KIC (acid form) exceeded 90 %.

An example preparation of [1–^{13}C]KIC with 30 mM EPA

To [1–^{13}C]KIC, 131 g/mol (100 µL, 100 mg) was added EPA (4.8 mg, 3.0 µmol)resulting in an EPA concentration of 30 mM.

Amount for small DNP sample: approximately 47 µL, 47 mg

Amount for large DNP sample: approximately 700 µL, 700 mg

100 % isotope labeled small DNP sample for 3.35T

To [1–^{13}C]KIC (100 µL, 100 mg) was added EPA to a final concentration of either 5 mM, 7.5 mM, 10 mM, 12.5 mM or 15 mM. Sample amounts corresponding to small DNP samples were transferred to sample cup and inserted into the polarizer.

100 % isotope labeled small DNP sample for 6.7T

To [1–^{13}C]KIC (100 µL, 100 mg) was added EPA to a final concentration of either 18 mM, 24 mM, 30 mM or 40 mM. Sample amounts corresponding to small DNP samples were transferred to sample cup and inserted into the polarizer.

10 % isotope labeled small DNP sample for 6.7T

[1–^{13}C]KIC (4.8 µL, 4.8 mg) was mixed withKIC (43.2 µL, 43.2 mg). To this mixture was added EPA (2.3 mg, 1.44 µmol AH111501). Resulting in an EPA concentration of 30 mM. Sample amount corresponding to small DNP samples was transferred to sample cup and inserted into the polarizer.

10 % isotope labeled large DNP sample for 6.7T

[1–^{13}C]KIC (70 µL, 70 mg) was mixed with KIC (630 µL, 630 mg). To this mixture was added EPA (33.5 mg, 21 µmol AH111501)resulting in an EPA concentration of 30 mM.

100 % isotope labeled large DNP sample for 6.7T

To [1–^{13}C]KIC (700 µL, 700 mg) was added EPA (33.5 mg, 21 µmol AH111501)resulting in an EPA concentration of 30 mM.

[1,4–^{13}C$_2$] fumaric acid

An example preparation of [1,4–^{13}C$_2$]FUM with 30 mM EPA

[1,4–^{13}C$_2$]FUM, 118 g/mol (110.5 mg, 0.936 mmol) was dissolved in DMSO (181 µl, 199 mg). This solution had a density of 1.20 and contained 3.0 mmol fumaric acid / g solution.

To 50 µL of this solution was added EPA (2.4 mg, 1.5 µmol)resulting in an EPA concentration of 30 mM.

Amount for small DNP sample: approximately 50 µL, 60 mg

Amount for large DNP sample: approximately 790 µL, 950 mg

100 % isotope labeled small DNP sample for 3.35T

[1,4–^{13}C$_2$]FUM (110.5 mg, 0.936 mmol) was dissolved in DMSO (181 µl, 199 mg). To aliquots of 50 µL of this solution was added EPA to a final concentration of either 5 mM, 8 mM, 11 mM, 13 mM or 16 mM. Sample amounts corresponding to small DNP samples were transferred to sample cup and inserted into the polarizer.

100 % isotope labeled small DNP sample for 6.7T

[1,4–^{13}C$_2$]FUM (110.5 mg, 0.936 mmol) was dissolved in DMSO (181 µl, 199 mg). To aliquots of 50 µL of this solution was added EPA to a final concentration of either 25 mM, 30 mM or 35 mM. Sample amounts corresponding to small DNP samples were transferred to sample cup and inserted into the polarizer.

10 % isotope labeled small DNP sample for 6.7T

[1,4–^{13}C$_2$]FUM (11 mg, 93 µmol) + FUM (99 mg, 0.853 mmol) was dissolved in DMSO (181 µl, 199 mg). To 50 µL of this solution was added EPA (2.4 mg, 1.5 µmol, AH111501) resulting in an EPA concentration of 30 mM.

10 % isotope labeled large DNP sample for 6.7T

[1,4–^{13}C$_2$]FUM (95 mg, 0.805 mmol) + FUM (855 mg, 7.37 mmol) was dissolved in DMSO (1562 µl, 1718 mg). To 790 µL of this solution was added EPA (37.8 mg, 23.7 µmol, AH111501) resulting in an EPA concentration of 30 mM.

For the [1,4–^{13}C$_2$]FUM formulation, quick sample loading into the polarizer cold space is essential to prevent sample crystallization. The equipment used in this study allows for this procedure as a routine practice.

Hyperpolarization using direct ^{13}C dDNP

All samples were hyperpolarized to equilibrium (3x T$_p$) at 3.35T and 1.3±0.05K in an original prototype polarizer [22] or at 6.7T and 1.3 ±0.05K in a SpinAligner [13]

At 6.7T microwave optimization was performed before hyperpolarization for each new type of sample formulation (DS1-DS4 and for each new MCA). See supporting information, Figure S5, for further information on Optimizing the microwave frequency for DNP.

All small samples were dissolved in phosphate buffer (50 mM, pH 7.4) with addition of adequate amounts of NaOH (10M) for pH neutralization.

All large samples were dissolved in Tris base (200 mM) with addition of adequate amounts of NaOH for pH neutralization and EDTA (to approximately 0.3 mM) for chelation of paramagnetic metal ions.

NMR analyses of polarization and T$_1$ were performed either on a Bruker Avance III 9.4 T spectrometer or on Magritek Spinsolve 1T or 1.4 T spectrometers

In vivo experiments

One healthy female Danish landrace pig (~40kg, 12 weeks) was anesthetized with propofol and fentanyl

(4–8, and 0.035 mg/kg/h IV) and ventilated with 40 % oxygen. A catheter was placed in the femoral artery and jugular vein under ultrasound guidance for invasive blood pressure monitoring, blood sampling and injections. All experiments were performed in accordance with relevant laws and ethics under permission from the Animal Experiment Inspectorate in Denmark.

[1–^{13}C]KIC and [1–^{13}C]PYR polarization protocol:

High concentration: 700 mg (5.3 mmol) [1–^{13}C]KIC and 420 mg (4.7mmol) [1–^{13}C]PYR with 30mM trityl EPA (AH111501)

Low concentration: 500 mg (3.8 mmol) [1–^{13}C]KIC and 300 mg (3.4mmol) [1–^{13}C]PYR with 30mM trityl EPA (AH111501)

Samples were polarized for ~1.5h and dissolved in 10mL dissolution medium with added NaOH for neutralization. Dissolution medium: Tris-buffer (200mM, pH 8.2), 0.27mM EDTA.

Directly after dissolution the samples were mixed with additional 20mL dissolution medium to a final HMCA volume of 30mL.

[1–^{13}C]KIC and [1–^{13}C]PYR signals were measured in the individual samples at 1.4T (Spinsolve, Magritek) and sample concentrations were measured with NMR on the individual HMCA adding ^{13}C-Urea as an internal standard.

HMCA injection:

30mL HMCA was injected intravenously in the femoral vein, followed by a 20mL flush with saline to empty the injection line. Four injections were made in the pig, in the following sequence: high concentration [1–^{13}C]KIC, low concentration [1–^{13}C]KIC, high concentration [1–^{13}C]PYR, low concentration [1–^{13}C]PYR.

MRS protocol:

^{13}C Acquisition

MR750 3T scanner (GE Healthcare, Waukesha, WI)

Carbon MRS was performed using an 8-channel flexible ^{13}C (/8ch Na) Rx coil [25] and a Clamshell Tx (RAPID Biomedical). Slice-selective MRS was performed starting at beginning of injection from an axial slice placed over the pig-head, including the whole brain. MR parameters for carbon spectroscopy were:

ST = 10cm, TR = 2s, FA = 10 deg, SBW = 5000Hz, spectral points = 2048, 60 spectra (TA = 2 min)

Proton MRI was obtained using standard, commercial coils. Routine T$_1$-weighted and T$_2$-weighted imaging was performed for planning of the ^{13}C-MRS.

Data analysis

NMR solid state T$_p$ and liquid state polarizations were analyzed from metabolite integrals measured using MestreNova software (MestreLab Research).

MRS metabolite peaks were fitted with an AMARES-based algorithm [26] using OXSA Matlab code, as previously described [27].

Apparent T$_1$ was calculated by fitting the [1–^{13}C]KIC and [1–^{13}C] PYR maximum amplitudes from timepoint 20s to a single term exponential model using MATLAB (version R2022b).

CRediT authorship contribution statement

Ditte B. Christensen: Writing – review & editing, Investigation, Formal analysis, Data curation, Conceptualization. **Ingeborg S. Skre:** Writing – original draft, Supervision, Resources, Project administration, Methodology, Investigation, Funding acquisition, Formal analysis, Data curation, Conceptualization. **Jan Henrik Ardenkjær-Larsen:** Writing – review & editing, Funding acquisition. **Magnus Karlsson:** Writing – review & editing, Investigation, Data curation, Conceptualization. **Mathilde H. Lerche:** Project administration, Investigation, Data curation, Conceptualization.

Declaration of competing interest

The authors declare that they have no known competing financial interests or personal relationships that could have appeared to influence the work reported in this paper.

Acknowledgement

The authors are grateful to the European Union's Horizon 2020 research and innovation programme ERC Synergy grant HyperQ (856432) and the Novo Nordisk Foundation (NNF 19Oc0055825) for supporting this work.

We would like to thank Frederik K. A. Paustian and Mads Magnus Hansen for initial work formulating KIC at 6.7T dDNP. We would also like to thank the MR group at Århus University Hospital, in particular Esben S.S. Hansen, Christoffer Laustsen, Markus P. Andersen, Duy Anh Dang and Nichlas V. Christensen, for sharing knowledge and supporting the pig experiments.

Supplementary materials

Supplementary material associated with this article can be found, in the online version, at doi:10.1016/j.jmro.2024.100184.

Data availability

Data will be made available on request.

References

[1] J. Kurhanewicz, D.B. Vigneron, J.H. Ardenkjaer-Larsen, J.A. Bankson, K. Brindle, C.H. Cunningham, F.A. Gallagher, K.R. Keshari, A. Kjaer, C. Laustsen, D. A. Mankoff, Hyperpolarized 13C MRI: path to clinical translation in oncology, Neoplasia 21 (1) (2019) 1–16.
[2] F.A. Gallagher, R. Woitek, M.A. McLean, A.B. Gill, R. Manzano Garcia, E. Provenzano, F. Riemer, J. Kaggie, A. Chhabra, S. Ursprung, J.T. Grist, K. Brindle, Imaging breast cancer using hyperpolarized carbon-13 MRI, Procee. National Acad. Sci. 117 (4) (2020) 2092–2098.
[3] L.M. Le Page, O.J. Rider, A.J. Lewis, V. Ball, K. Clarke, E. Johansson, C.A. Carr, L. C. Heather, D.J. Tyler, Increasing pyruvate dehydrogenase flux as a treatment for diabetic cardiomyopathy: a combined 13C hyperpolarized magnetic resonance and echocardiography study, Diabetes 64 (8) (2015) 2735–2743.
[4] A.D. Sherry, C.R. Malloy, New Insights into Metabolic Regulation from Hyperpolarized 13C MRS/MRI Studies. Dynamic Hyperpolarized Nuclear Magnetic Resonance, Springer International Publishing, Cham, 2021, pp. 181–203.
[5] M. Karlsson, P.R. Jensen, J.Ø. Duus, S. Meier, M.H. Lerche, Development of dissolution DNP-MR substrates for metabolic research, Appl. Magn. Reson. 43 (2012) 223–236.
[6] M.M. Chaumeil, C. Najac, S.M. Ronen, Studies of metabolism using 13C MRS of hyperpolarized probes, Methods Enzymol. 561 (2015) 1–71.
[7] K. Golman, J.S. Petersson, P. Magnusson, E. Johansson, P. Åkeson, C.M. Chai, G. Hansson, S. Månsson, Cardiac metabolism measured noninvasively by hyperpolarized 13C MRI, Magn Reson Med 59 (5) (2008) 1005–1013.
[8] R.S. Tougaard, E.S.S. Hansen, C. Laustsen, J. Lindhardt, M. Schroeder, H.E. Bøtker, W.Y. Kim, H. Wiggers, H. Stødkilde-Jørgensen, Acute hypertensive stress imaged by cardiac hyperpolarized [1-13C] pyruvate magnetic resonance, Magn. Reson. Med. 80 (5) (2018) 2053–2061.
[9] http://Clinicaltrials.gov/ accessed: 31 July 2024.
[10] M. Karlsson, P.R. Jensen, R. in't Zandt, A. Gisselsson, G. Hansson, J.Ø. Duus, S. Meier, M.H. Lerche, Imaging of branched chain amino acid metabolism in tumors with hyperpolarized 13C ketoisocaproate, Int. J. Cancer 127 (3) (2010) 729–736.
[11] S.A. Butt, L.V. Søgaard, P.O. Magnusson, M.H. Lauritzen, C. Laustsen, P. Åkeson, J. H. Ardenkjær-Larsen, Imaging cerebral 2-ketoisocaproate metabolism with hyperpolarized 13C magnetic resonance spectroscopic imaging, J. Cereb. Blood Flow. Metabol. 32 (8) (2012) 1508–1514.
[12] F.A. Gallagher, M.I. Kettunen, D.E. Hu, P.R. Jensen, R.I.T. Zandt, M. Karlsson, A. Gisselsson, S.K. Nelson, T.H. Witney, S.E. Bohndiek, G. Hansson, T. Peitersen, M. H. Lerche, K. brindle, Production of hyperpolarized [1, 4-13C2] malate from [1, 4-13C2] fumarate is a marker of cell necrosis and treatment response in tumors, in: Proceedings of the National Academy of Sciences 106, 2009, pp. 19801–19806.
[13] J.H. Ardenkjær-Larsen, S. Bowen, J.R. Petersen, O. Rybalko, M.S. Vinding, M. Ullisch, N.C. Nielsen, Cryogen-free dissolution dynamic nuclear polarization polarizer operating at 3.35 T, 6.70 T, and 10.1 T, Magn. Reson. Med. 81 (3) (2019) 2184–2194.
[14] J.H. Ardenkjaer-Larsen, A.M. Leach, N. Clarke, J. Urbahn, D. Anderson, T. W. Skloss, Dynamic nuclear polarization polarizer for sterile use intent, NMR Biomed. 24 (8) (2011) 927–932.
[15] A. Capozzi, S. Patel, W.T. Wenckebach, M. Karlsson, M.H. Lerche, J.H. Ardenkjær-Larsen, Gadolinium effect at high-magnetic-field DNP: 70 % 13C polarization of [U-13C] glucose using trityl, J. Phys. Chem. Lett. 10 (12) (2019) 3420–3425.
[16] A. Comment, J. Rentsch, F. Kurdzesau, S. Jannin, K. Uffmann, R.B. Van Heeswijk, P. Hautle, J.A. Konter, B. Van den Brandt, J.J. Van der Klink, Producing over 100 ml of highly concentrated hyperpolarized solution by means of dissolution DNP, J. magnetic reson. 194 (1) (2008) 152–155.
[17] T. Cheng, A.P. Gaunt, I. Marco-Rius, M. Gehrung, A.P. Chen, J.J. van der Klink, A. Comment, A multisample 7 T dynamic nuclear polarization polarizer for preclinical hyperpolarized MR, NMR Biomed. 33 (5) (2020) e4264.
[18] T.P. Lê, J.N. Hyacinthe, A. Capozzi, Multi-sample/multi-nucleus parallel polarization and monitoring enabled by a fluid path technology compatible cryogenic probe for dissolution dynamic nuclear polarization, Sci. Rep. 13 (1) (2023) 7962.
[19] K. Golman, R. in 't Zandt, M. Thaning, Real-time metabolic imaging, in: Proceedings of the National Academy of Sciences 103, 2006, pp. 11270–11275.
[20] J.H. Ardenkjær-Larsen, S. Macholl, H. Johannesson, Dynamic nuclear polarization with trityls at 1.2 K, Appl. Magn. Reson. 34 (3) (2008) 509–522.
[21] H.A. Yoshihara, E. Can, M. Karlsson, M.H. Lerche, J. Schwitter, A. Comment, High-field dissolution dynamic nuclear polarization of [1-13 C] pyruvic acid, Phys. Chem. Chem. Phys 18 (18) (2016) 12409–12413.
[22] J.H. Ardenkjær-Larsen, B. Fridlund, A. Gram, G. Hansson, L. Hansson, M.H. Lerche, R. Servin, M. Thaning, K. Golman, Increase in signal-to-noise ratio of>10,000 times in liquid-state NMR, in: Proceedings of the National Academy of Sciences 100, 2003, pp. 10158–10163.
[23] J.W. Gordon, H.Y. Chen, N. Dwork, S. Tang, P.E. Larson, Fast imaging for hyperpolarized MR metabolic imaging, J. Magnetic Reso. Imaging 53 (3) (2021) 686–702.
[24] M.E. Conway, S.M. Hutson, BCAA metabolism and NH 3 homeostasis, Glutamate/GABA-Glut. Cycle. Amino Acid Neurot. Homeost. (2016) 99–132.
[25] J.D. Sanchez-Heredia, R.B. Olin, J.T. Grist, W. Wang, N. Bøgh, V. Zhurbenko, E. S. Hansen, R.F. Schulte, D. Tyler, C. Laustsen, J.H. Ardenkjær-Larsen, RF coil design for accurate parallel imaging on 13C MRSI using 23Na sensitivity profiles, Magn. Reson. Med. 88 (3) (2022) 1391–1405.
[26] L Vanhamme, A van den Boogaart, S. Van Huffel, Improved method for accurate and efficient quantification of MRS data with use of prior knowledge, J. Magn. Reson. 129 (1) (1997) 35–43.
[27] LAB Purvis, WT Clarke, L Biasiolli, L Valkovic, MD Robson, CT. Rodgers, OXSA: An open-source magnetic resonance spectroscopy analysis toolbox in MATLAB, PLoS. One 12 (9) (2017) e0185356.